



Evaluation the Effect of Silica Nanoparticles and Ultraviolet Process on Deoxynivalenol Detoxification in Sunflower Oils

Neda Ghaffari¹, Ehsan Sadeghi*², Nasrin Choobkar³

1- Food Department, Kermanshah Branch, Islamic Azad University, Kermanshah, Iran

2- Research Center for Environmental Factors Affecting Health, Kermanshah University of Medical Sciences, Kermanshah, Iran

3- Plant Biotechnology Research Center, Kermanshah Branch, Islamic Azad University, Kermanshah, Iran

ARTICLE INFO

Article History:

Received:2024/3/5

Accepted:2024/7/3

Keywords:

Silica Nanoparticles,

Zearalenone,

Sunflower Oil,

UV Radiation,

Adsorption

DOI: 10.22034/FSCT.21.157.31.

*Corresponding Author E-
ehsan.sadeghi59@yahoo.com

ABSTRACT

In this study, the effect of silica nanoparticles (SNPs) and UV radiation on the removal of zearalenone (ZEN) from sunflower oil was investigated. Pure sunflower oil samples showed no contamination with ZEN. The optimal conditions for ZEN removal using SNPs were determined to be a contact time of 240 minutes, an initial ZEN concentration of 25 µg/L, and 4 mg of SNPs. The kinetic data conformed to the Freundlich model and pseudo-second-order model. The results showed that SNPs have a high adsorption capacity and act as an effective adsorbent for removing ZEN from sunflower oil. The effect of SNPs in reducing ZEN was significantly more effective than UV radiation. The probable adsorption mechanism includes the chemical bonding of ZEN functional groups with silica groups and the high porosity of SNPs. Due to the low cost and non-toxic nature, the use of SNPs was introduced as an effective method for ZEN removal from food products. This method can be utilized as an efficient approach for ZEN removal in natural samples like edible oil.

1- Introduction

Food safety plays a crucial role in human life. Mycotoxins are toxic secondary metabolites produced by a wide range of fungi, and their growth poses a threat to human life. Due to their structural diversity and varying physical properties, mycotoxins cause a broad spectrum of biological effects, including genotoxicity, mutagenicity, carcinogenicity, teratogenicity, and toxic effects on the kidneys, liver, skin, nervous system, and more [1, 2]. Mycotoxins are small and highly stable molecules, making their removal or eradication very difficult. They enter the food chain while retaining their toxic properties. Given the toxicity of mycotoxins and the serious risks they pose to humans and animals, controlling all stages from farm to consumer is essential to minimize mycotoxin production. Aflatoxin B1 (AFB1), Fumonisin B1 (FB1), Deoxynivalenol (DON), Ochratoxin A (OTA), and Zearalenone (ZEN) are the five main mycotoxins causing major contamination in agricultural products and foods, creating some of the most problematic fungal contamination issues in crops [3, 4].

ZEN is a non-steroidal and estrogenic mycotoxin produced by several *Fusarium* species such as *Fusarium graminearum* and *Fusarium culmorum*. It functions as an endocrine disruptor in mammals [5]. As an estrogenic mycotoxin, ZEN can mimic the hormone estrogen in the body, leading to hormonal imbalances in individuals, especially women and girls. Due to its estrogenic effects, ZEN can cause hormonal disorders, reduced sperm quality, fetal malformations, and even severe damage to the nervous system, liver, and immune system. Consumption of ZEN-contaminated food can seriously harm human and animal health, making the control and removal of this mycotoxin from food products highly important. If ZEN is

not eliminated during production, it affects the food chain through various food products including corn, wheat, barley, oats, and more. Edible oils, plant-based oils, nuts, spices, milk, eggs, meat, fermented products, beverages, and even drinking water can be exposed to this toxin [6, 7].

The Food and Agriculture Organization (FAO) has reported that ZEN contamination in various food products ranges from 50 to 1000 micrograms per kilogram, with higher regulatory levels for corn products [6]. In many countries, the maximum allowable level of ZEN in food for human consumption is set between 20 and 1000 micrograms per kilogram [6]. Due to inadequate processing and storage conditions, agricultural products used for oil extraction are recognized as potential environments for fungal growth and mycotoxin production, including ZEN [8].

Removing the mycotoxin zearalenone (ZEN) from edible oils presents several technical and operational challenges that require effective and efficient approaches. These challenges include: Firstly, ZEN, being a highly heat-stable mycotoxin, resists complete degradation through thermal methods, necessitating the use of methods that can counteract its thermal stability [9]. Secondly, during ZEN removal processes, there is a risk of transferring the mycotoxin to other products, which could lead to its loss, thus the use of safe and efficient methods is crucial. Thirdly, ZEN is sensitive to specific physical and chemical conditions, requiring precise conditions for its removal, such as pH, temperature, contact time, and concentration of absorbents. Fourthly, selecting an appropriate method for ZEN removal requires a careful assessment of process efficiency and yield, with considerations for lower costs and environmental sustainability. Finally, using absorbent materials with the ability to capture ZEN involves complex processes and equipment, making the choice of stable and effective absorbents a fundamental challenge in this field [10].

Efforts to remove or reduce ZEN using various methods have been extensive [11]. Edible additives and inert absorbents have shown the

most promise in reducing the toxic effects of ZEN. UV radiation is also employed as a method for detoxifying edible oils before packaging and degrading toxins in foods. This detoxification process is efficient, rapid, sustainable, and cost-effective, while minimizing the loss of nutrients, color, and flavor of the product [12].

In recent years, the use of nanomaterials, including polymers, metallic nanoparticles (MeNPs), quantum dots (QDs), carbon nanotubes (CNTs), and magnetic nanoparticles (MNPs), as absorbents for removing mycotoxins from food has attracted considerable attention for developing new detoxification processes. Nanomaterials and nanoparticles, due to their high surface-to-volume ratio, can bind to higher concentrations of mycotoxins. Additionally, nanoparticles can modify various functional groups using specific ligands or surface coatings [6].

To utilize silica nanoparticles as absorbents for removing ZEN from edible oils, the following characteristics and properties are crucial: Firstly, silica nanoparticles have a high surface area and a coated surface structure, which increases the contact between the nanoparticles and ZEN in edible oils, enhancing the likelihood of contaminant absorption. Secondly, the high loading capacity of silica nanoparticles improves their ability to absorb and retain ZEN, reducing the need for frequent replacement of the absorbent [13]. Thirdly, due to their structure, silica nanoparticles exhibit high stability under various conditions such as temperature, pH, and corrosion, which helps maintain their adsorption performance over time. Fourthly, silica nanoparticles can adjust their adsorption and transfer properties through different surface coatings, increasing their selectivity for ZEN. Lastly, the uniform and homogeneous structure of silica nanoparticles ensures even and optimal distribution and absorption of contaminants, which improves the effectiveness of ZEN removal from edible oils. Given these features, silica nanoparticles are proposed as suitable absorbents for ZEN removal from edible oils, potentially aiding in the effective control of mycotoxin contamination in food products [14, 15].

Ultraviolet (UV) radiation has emerged as an effective physical method for removing mycotoxins from food, especially for ZEN.

This method utilizes UV radiation to break the chemical bonds of ZEN, reducing its toxic activity and mitigating health risks. UV radiation can significantly reduce the toxicity of ZEN and protect food contaminated with this mycotoxin. The economic and operational advantages of this method include its efficiency and speed in removing ZEN, reduction of waste, increased production yield, and the use of a sustainable, low-energy technology. Overall, UV radiation represents an efficient and sustainable approach for ZEN removal from food, offering significant economic and environmental benefits while improving food quality and safety [16].

In studies related to mycotoxins, particularly zearalenone, models and kinetics have been recognized as vital tools for analyzing and predicting the removal and degradation processes of these contaminants by external agents. In this research, mathematical and kinetic models were used to examine the process of ZEN removal under the influence of silica nanoparticles and UV radiation [17]. Models such as the Langmuir and Freundlich models were employed to determine the rate of ZEN removal under various conditions. These models assist in accurately and quantitatively analyzing the performance of silica nanoparticles and UV radiation in ZEN removal, and improving the mechanisms involved in ZEN detoxification through data analysis techniques. These studies highlight that mathematical and kinetic models not only enhance the understanding of ZEN removal processes but are also crucial for advancing mycotoxin detoxification technologies [18].

Several studies have investigated the effectiveness of silica nanoparticles as efficient adsorbents for the removal of mycotoxins. For example, Raesi and colleagues (2022) examined the effect of ZnO nanoparticles on the removal of aflatoxin B1 (AFB1) from aqueous solutions under UV light. They found that using 0.10 mg/mL ZnO for 60 minutes achieved complete removal of AFB1 with an initial concentration of 10 µg/L. The results indicated that this process was consistent with a pseudo-first-order model and Langmuir isotherm, suggesting that ZnO nanoparticles can be an effective method for detoxifying AFB1 in liquid food products [19]. Nicolau-Lapeña also explored the use of UV-C (254 nm)

radiation for reducing patulin in apple-derived products and juices. Their results showed that UV irradiation with energies of 8.8 (UV-1) and 35.1 (UV-2) kJ m^{-2} was effective in eliminating *Penicillium expansum* CMP-1 spores on apple surfaces [20]. Additionally, Garcia and colleagues (2023) used kinetic models to study aflatoxin production by *Aspergillus flavus* in maize agar and maize kernels. Their findings indicated that colony size/area, dry biomass weight, and aflatoxin accumulation were directly related, and the Luedeking–Piret model was used to model AFB1 production [21].

To date, no research has been conducted on the simultaneous use of silica nanoparticles and UV radiation for the removal of zearalenone from sunflower oils. Therefore, the primary objective of this study is to investigate and compare the effects of these two factors on the efficiency of zearalenone removal from sunflower oils. This research aims to explore the mechanisms of zearalenone adsorption and degradation under various conditions of time, concentration, and silica nanoparticle amounts, with the goal of optimizing the removal process and improving its efficiency in real food environments.

2- Materials and Methods

2-1- Materials

Standard ZEN powder was purchased from Sigma-Aldrich (USA). Formic acid (HCOOH), tetraethyl orthosilicate (TEOS), methanol, and

acetonitrile were obtained from Merck (Germany). The analytical reagents and chemicals used in this study were employed without additional purification. Methanol, HCOOH, acetonitrile, and distilled water were used as solvents. Distilled water served as the mobile phase in HPLC and as a solvent for preparing solutions.

2-2- HPLC Analysis

ZEN was measured in triplicate using an Azura HPLC system (Germany) equipped with a Shimadzu RF-20A fluorescence detector (Japan) and post-column photochemical derivatization with an LCTech GmbH model (Germany). The HPLC system consisted of a C18 analytical column (250 mm \times 4.6 mm, 5 μm particle size) with a pre-column, maintaining the column temperature at 40°C. Acetonitrile and water in a ratio of 80:20 (v/v) were used as the mobile phase at a flow rate of 0.1 mL/min. The excitation and emission wavelengths of the fluorescence detector were set to 274 nm and 440 nm, respectively. The injection volume for both standard and sample solutions was 20 μL .

The ZEN stock solution (10 mg/L) was prepared by dissolving ZEN in methanol/water (80:20, v/v) with 1% HCOOH, and the solutions were stored at -20°C. Figure 1 shows the chromatogram of the standard ZEN solution at a concentration of 10 mg/L.

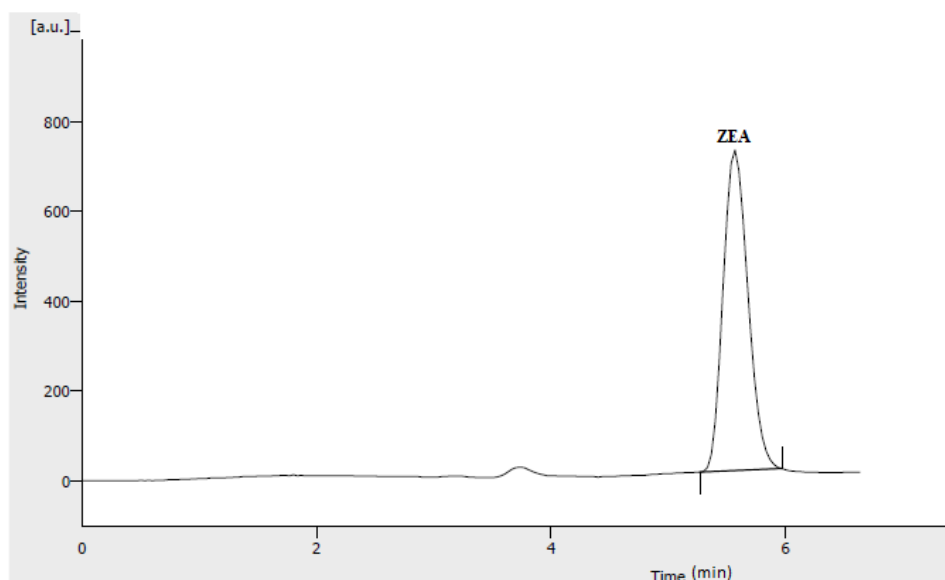


Fig 1 HPLC chromatogram of ZEN standard at 10 mg/L concentration

2-3- Synthesis of Silica Nanoparticles (SNPs)

There are various methods for synthesizing silica nanoparticles (SNPs). The precursors used for the synthesis of SNPs are typically alkoxide precursors such as tetraethyl orthosilicate (TEOS) and tetramethyl orthosilicate (TMOS), or metal salt precursors like sodium silicate. These materials react with water in both acidic and basic environments to ultimately form silica gel. In practice, acid and base are used as catalysts to drive the reaction. The silica gel formation process consists of two stages: In the first stage, the alkoxide precursor

reacts with water to form silanol groups (hydrolysis). In the second stage, the silanol groups formed in the first stage react with each other to form silica gel (condensation) [22]. SNPs were prepared based on a previously reported method [23]. The synthesis of SNPs in this study begins by dissolving 1 mL of TEOS and 3 mL of hydrochloric acid in 25 mL of deionized water at room temperature. A solution made from 2 mL of TEOS and 10 mL of urea (9 M) is then slowly added to the previous solution. This new solution is maintained at 40°C for 7 days. Finally, the solution is heated at 600°C for 2 hours to obtain the silica nanoparticles. Figure 2 illustrates the stages of SNPs preparation.

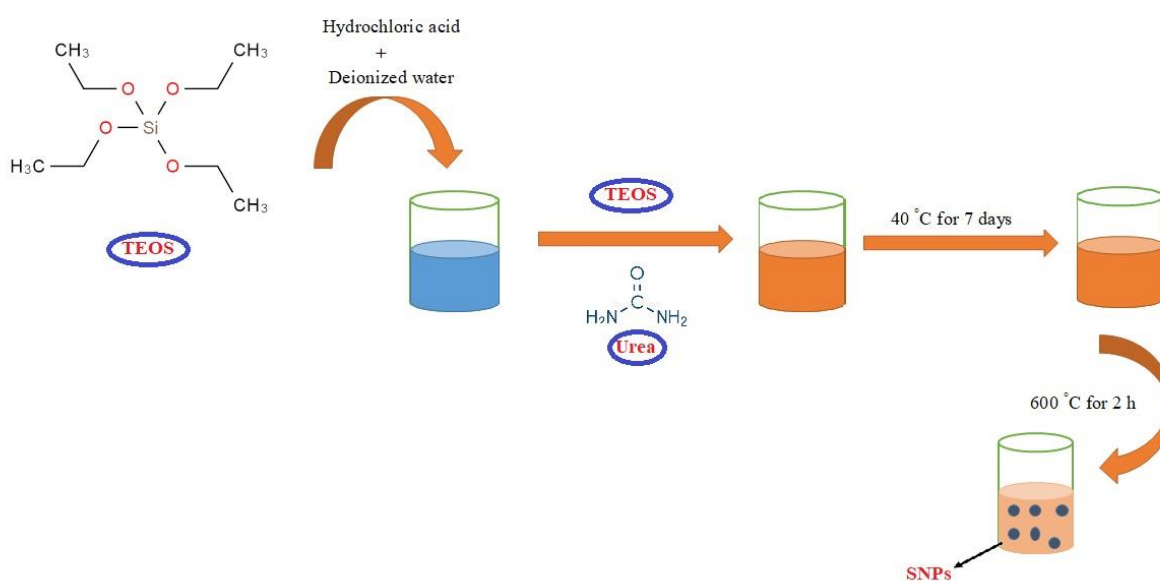


Fig 2 The pathway of synthesis of SNPs.

2-4- ZEN Adsorption Process

Adsorption experiments were conducted by adding a specified amount of SNPs as an adsorbent to 10 mL of ZEN solution with varying concentrations. To evaluate the effect of contact time on ZEN removal, experiments were performed at time intervals ranging from 10 to 300 minutes in a 50:50 v/v methanol/water mixture and 1% HCOOH solution. The ZEN solutions were centrifuged at 6000 rpm for 10 minutes at the designated contact times, after which the supernatant was filtered through a 0.2-micrometer pore size

filter paper. The residual ZEN concentration was measured using HPLC.

After optimizing the contact time, the initial ZEN concentration (ranging from 25 to 125 µg/L) and the amount of SNPs (ranging from 0 to 8 mg) were varied. The adsorption of ZEN by SNPs was evaluated using two parameters: adsorption capacity (q) and removal percentage (R%), which can be calculated using the following equations [22]:

$$\text{ZEN Removal Percentage (R\%)} = \frac{C_0 - C_t}{C_0} \times 100 \quad (\text{eq.1})$$

$$\text{Equilibrium Adsorption Capacity (} q_e \text{)} = \frac{(C_0 - C_t)V}{C_0 W} \times 100 \quad (\text{eq.2})$$

In the above equations, %R represents the percentage removal of ZEN and C_t denote the initial and final concentrations of ZEN in $\mu\text{g/L}$, respectively, q_e is the adsorption capacity at equilibrium in $\mu\text{g/g}$, V is the volume of the solution in mL, and W is the weight of the adsorbent (SNPs) in mg.

2-5- Detoxification of ZEN Using UV Radiation

In this experiment, 10 mL of a 50:50 (v/v) methanol/water mixture and 1% HCOOH solution containing 100 $\mu\text{g/L}$ ZEN was placed in a test tube and exposed to direct UV radiation at a distance of 10 cm from a 15-watt UV lamp for durations ranging from 0 to 360 minutes. After centrifuging the samples at 6000 rpm for 10 minutes and filtering the solution through a 0.2 μm filter paper, the residual ZEN concentration was measured using HPLC. To evaluate the effect of UV radiation on ZEN removal, the percentage removal of ZEN (RR%R) was calculated using Equation (1).

2-6- Kinetic Study of Adsorption

To study the kinetics of ZEN adsorption by silica nanoparticles (SNPs), standard ZEN solutions with concentrations of 10, 20, 30, 40, and 50 mg/L were prepared at a constant temperature of 25°C. A specific amount of silica nanoparticles was added to each of these solutions, and samples were taken at various time intervals (1, 5, 10, 20, 30, 60, 120, and 180 minutes). The residual ZEN concentration in each sample was measured using UV-Vis spectrophotometry at a wavelength of 274 nm. The obtained data were analyzed to determine the kinetic parameters, including the adsorption rate constant (k) and equilibrium adsorption capacity (q_e), using pseudo-first-order and pseudo-second-order kinetic models. These analyses were performed using OriginPro version 2021 (OriginLab Corporation,

USA) to identify the best kinetic model describing the adsorption process of ZEN by silica nanoparticles [24].

2-6. Detoxification of ZEN in Sunflower Oil

This section describes the process of detoxifying ZEN in sunflower oil using silica nanoparticles (SNPs) and UV irradiation. Sunflower oil samples were contaminated with specific concentrations of ZEN, and the effects of SNPs and UV radiation on ZEN removal were evaluated.

2-6-1. Adsorption of ZEN by SNPs

To investigate ZEN adsorption by silica nanoparticles (SNPs), sunflower oil samples were prepared with varying concentrations of ZEN (25, 50, 75, and 100 $\mu\text{g/L}$). Different amounts of SNPs (1, 2, 3, 4, and 5 mg) were added to 10 mL of these samples. The samples were kept at room temperature for various time intervals (30, 60, 120, 180, and 240 minutes) and then centrifuged at 6000 rpm for 10 minutes. The supernatant was filtered, and the residual concentration of ZEN was measured using HPLC.

2-7. Fourier-Transform Infrared Spectroscopy (FTIR)

To investigate the chemical interactions between ZEN and silica nanoparticles (SNPs), Fourier-transform infrared spectroscopy (FTIR) was employed. Samples of SNPs, ZEN, and ZEN adsorbed onto SNPs were prepared, and their FTIR spectra were recorded in the range of 4000-400 cm^{-1} using a FTIR spectrometer (Bruker Vertex 70, USA). Changes in characteristic absorption bands, particularly in regions related to hydroxyl, carbonyl, and silicate functional groups, were analyzed.

2-8. Scanning Electron Microscopy (SEM)

Scanning electron microscopy (SEM) was used to examine the morphology and size of silica nanoparticles (SNPs) and the effect of ZEN adsorption on their surface. The samples were coated with a thin layer of gold to enhance electrical conductivity. SEM images were obtained using a scanning electron microscope model MIRA3 (Tescan, Czech Republic).

2-9. Statistical Analysis

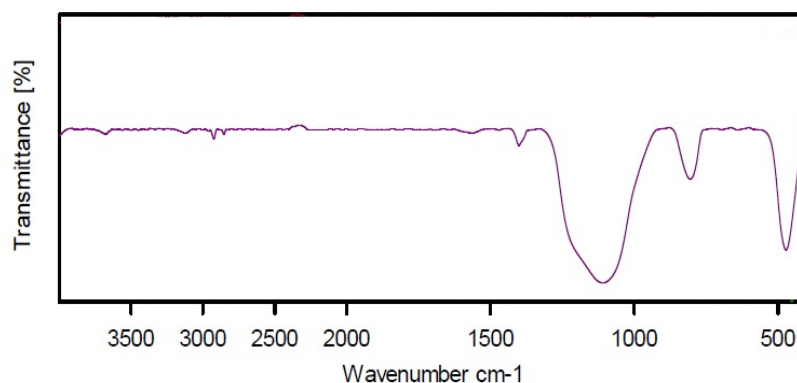
Data were analyzed and compared using SPSS software version 21 (USA). All adsorption experiments were performed in triplicate, with HPLC analysis conducted in duplicate. Experimental data are reported as means and standard deviations for three replicates. The mean \pm 95% confidence interval was used to identify significant differences between means in each experiment. One-way ANOVA at a 95% confidence level was employed to compare all results, and significance was determined for each mean value ($P < 0.05$).

3-Results and Discussion

3-1. Characterization of SNPs

The FT-IR spectrum of the SNPs is shown in Figure 3. A strong, broad peak at 1107 cm^{-1} corresponds to the asymmetric stretching vibrations of the Si-O-Si bonds. The peaks observed at 801 cm^{-1} and 469 cm^{-1} can be attributed to the symmetric stretching and bending vibrations of the Si-O-Si bonds, respectively. These findings are consistent with previous reports on the characteristic peaks of silica [22].

SEM was used to assess the surface characteristics of the synthesized SNPs. Figure 4 shows the SEM image of the SNPs. As observed, the silica particles are aggregated in clusters of varying sizes, ranging from 47 to 68 nanometers. The clustering of these particles results in the formation of a continuous network, giving the particles a gel-like appearance. The clusters influence the size of surrounding clusters, and consequently, their density is limited by the number of clusters [22].



FT-IR spectra of SNPs **Fig 3**

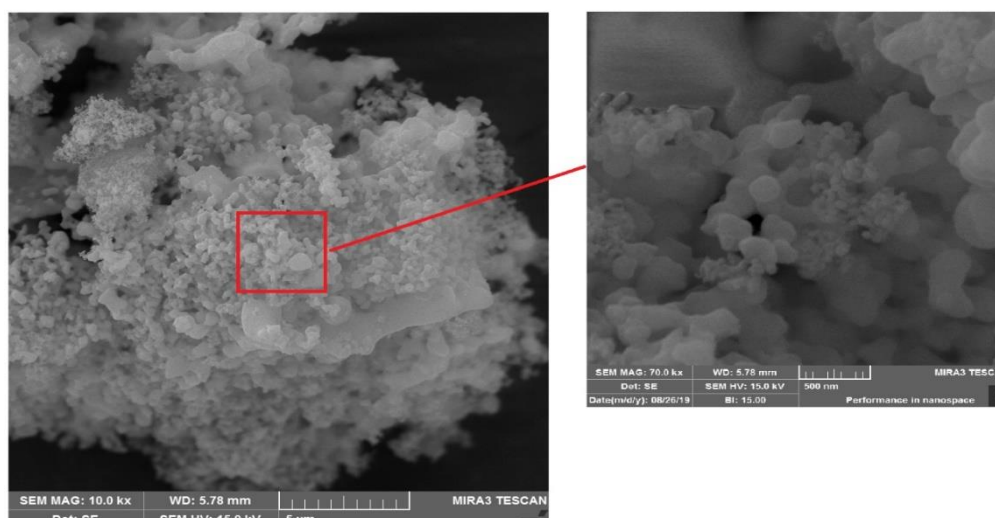


Fig 4 SEM image of synthesized SNPs.

3-2. Method Validation

HPLC with a fluorescence detector was chosen for the analysis and identification of ZEN [22]. The linear regression equation, $y=1.0317x+32.782y = 1.0317x + 32.782y=1.0317x+32.782$, was obtained for the ZEN standard curve with a correlation coefficient of 0.9978, based on the linear relationship between peak area and different concentrations of ZEN (5, 25, 50, 75, and 100 $\mu\text{g/L}$).

To evaluate the precision and accuracy of the method experimentally, concentrations of 25 and 50 $\mu\text{g/L}$ of ZEN were injected into sunflower oil samples. The mean recovery rates and relative standard deviations (RSD), based on triplicate measurements ($n=3$), were calculated as 96.23% and 3.74% for 25 $\mu\text{g/L}$ ZEN, and 94.07% and 3.15% for 50 $\mu\text{g/L}$ ZEN, respectively. These results indicated that the method is reliable for determining ZEN in real samples.

The limit of quantification (LOQ) and the limit of detection (LOD) were determined as 2 $\mu\text{g/L}$ and 0.5 $\mu\text{g/L}$, respectively, based on achieving signal-to-noise ratios (S/N) ≥ 3

for LOD and (S/N) ≥ 6 for LOQ, which are largely influenced by the detector used [22].

3-3. Effect of Contact Time on ZEN Adsorption

To examine the effect of contact time on ZEN adsorption, removal experiments were conducted with 25 $\mu\text{g/L}$ ZEN solution over a time range of 10 to 300 minutes at room temperature. The results are presented in Figure 5. As contact time increased, the removal of ZEN on the surface of SNPs also increased, with equilibrium achieved after 240 minutes. The removal rate of ZEN initially rose rapidly until a specific time point, after which it increased more slowly as equilibrium was approached. Beyond 240 minutes, there was no significant change in adsorption capacity.

Accordingly, the optimal contact time for adsorption equilibrium was determined to be 240 minutes for ZEN, indicating that the rapid adsorption of ZEN by SNPs is due to the presence of active functional groups, larger surface area, and high porosity on the surface of SNPs. These factors facilitate the rapid diffusion of ZEN molecules from the solution onto the adsorbent surface [22].

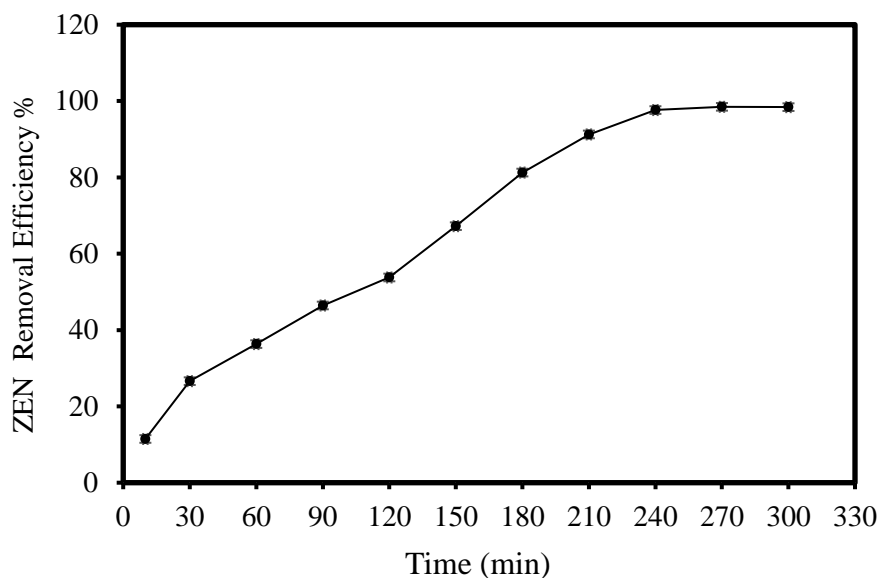


Fig 5 Effect of contact time on ZEN removal efficiency

in adsorbent mass. As a result, the maximum removal efficiency for ZEN was achieved at a concentration of 25 $\mu\text{g/L}$.

3-4. Effect of Initial Concentration on ZEN Adsorption

The effect of the initial concentration of ZEN on the removal efficiency was evaluated within a concentration range of 25 to 125 $\mu\text{g/L}$, as shown in Figure 6A. The removal efficiency significantly decreased as the ZEN concentration increased up to 125 $\mu\text{g/L}$. As the ZEN concentration in the aqueous solution increased, the adsorption efficiency decreased further. This is because, with higher ZEN concentrations in the solution, the number of ZEN molecules increases without a corresponding increase

In dilute solutions, the mobility of ZEN molecules is higher, leading to greater interaction and a stronger affinity of SNPs for ZEN molecules. For initial ZEN concentrations of 25 and 125 $\mu\text{g/L}$, the average removal efficiencies were 97.64% and 83.82%, respectively, with standard deviations of 0.51 and 0.99. These results indicate a significant difference between the concentrations ($P < 0.05$).

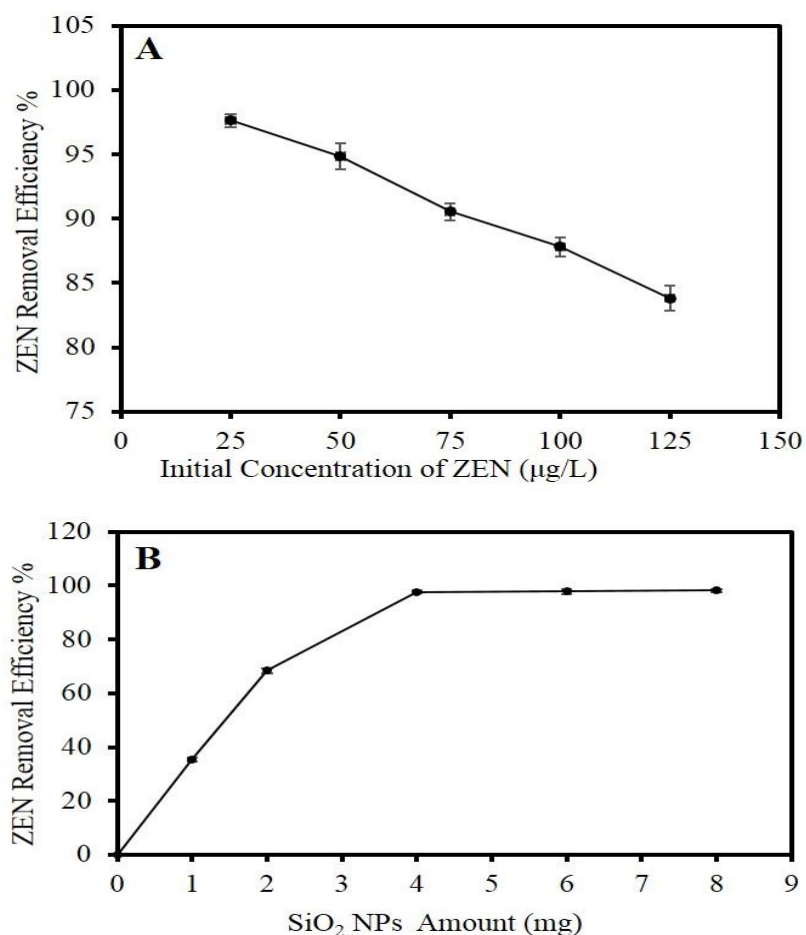


Fig 6 Effect of initial concentration of ZEN (A) and SNPs (B) on ZEN removal efficiency

3-5. Effect of SNP Amount on ZEN Adsorption

Figure 6B illustrates the effect of varying the amount of SNPs on ZEN adsorption. In this stage, the removal of ZEN by SNPs was studied using different adsorbent amounts ranging from 0 to 8 mg. As a result, the ZEN removal efficiency increased with SNP amounts up to 4 mg, leading to a larger adsorbent surface area and enhanced adsorption processes. However, after adding more SNPs, the removal efficiency remained almost unchanged. The increased amount of SNPs in the solution may lead to adsorbent aggregation, which could reduce the effective adsorption sites and, thus, diminish adsorption efficiency. Therefore, increasing the adsorbent dose beyond a

certain point may not further improve the removal efficiency. The maximum removal efficiency was achieved with 4 mg of SNPs, making this the optimal amount for ZEN adsorption.

Currently, mycotoxin adsorbents are the most direct, practical, and feasible way to reduce ZEN contamination in food. Various types of mycotoxin adsorbents are commonly used in the market. For example, the addition of small percentages of antifungal agents (such as sorbic acid, benzoic acid, calcium propionate, and propionic acid) can significantly reduce contamination. However, the quality of these adsorbents varies, and there is no unified national standard for them. Therefore, there is a critical need to develop specific evaluation methods for assessing

the detoxification effects of mycotoxin adsorbents .

Savi et al. (2023) demonstrated that mesoporous silica nanoparticles (MSN) have a strong ability to adsorb aflatoxin B1 (AFB1). Their results showed that with an MSN concentration of 0.1 mg/mL, the AFB1 adsorption capacity reached 30%, and with an increase in concentration to 2 mg/mL, it increased to 70%. These nanoparticles adsorbed about 67% of AFB1 in a short time (around 15 minutes), and their adsorption capacity remained stable in the solution .

3-6. Kinetic Study of Adsorption

Adsorption is one of the most important and widely used methods due to its relatively simple design, cost-effectiveness, and energy efficiency . To study the experimental results, pseudo-first-order and pseudo-second-order models were employed to examine the adsorption process and evaluate the adsorption kinetic mechanism . These models were used to investigate the mechanism of adsorption and the rate-controlling steps, such as mass transfer and chemical reaction processes. It was assumed that the reaction order and rate constant would be determined by experimental data.

These two models have been applied across a wide range of adsorption systems, from biomass to nanomaterials as adsorbents. Analyzing equilibrium conditions is crucial for assessing the affinity or capacity of an adsorbent. Therefore, it is important to determine how the adsorption rate depends on the concentration of both the adsorbent and adsorbate in a solution and how the adsorption rate is influenced kinetically by the adsorption capacity or characteristics of the adsorbent.

These models are represented by Equation 3 for the pseudo-first-order model and

Equation 4 for the pseudo-second-order model:

$$\ln (q_e - q_t) = \ln q_e - k_1 t \quad (3)$$

$$t/q_t = 1/k_2 q_e^2 + t/q_e \quad (4)$$

where q_e , representing the amount of ZEN at equilibrium in micrograms per gram, q_t , the amount of ZEN at any time in micrograms per gram, k_1 , the pseudo-first-order rate constant in min^{-1} , and k_2 , the pseudo-second-order rate constant in $\text{g} \cdot \mu\text{g}^{-1} \text{min}^{-1}$, were obtained. Based on the linear plot of $\ln (q_e - q_t)$ versus t in Equation 3 (Figure A7) and t/q_t versus t in Equation 4 (Figure B7), the parameters q_e , k_1 , and k_2 were calculated. The value of q_e was determined to be 61.02 $\mu\text{g/g}$.

As shown, the correlation coefficient of the pseudo-first-order kinetic model for ZEN adsorption is lower than that of the pseudo-second-order model. These results indicate that the pseudo-second-order model describes the kinetics of ZEN adsorption onto SNPs more accurately than the pseudo-first-order model. Hence, the pseudo-second-order model was used, demonstrating that the adsorption rate depends not on the concentration of the adsorbate but rather on the adsorption capacity [22]. If the kinetic model closely fits the pseudo-first-order model, it suggests that the reaction tends to favor physical adsorption (a diffusion-controlled process). Conversely, if the reaction aligns well with the pseudo-second-order model, it implies a preference for chemical adsorption (adsorption reactions at the liquid/solid interface of the adsorbent) [22]. Table 1 presents the calculated kinetic parameters. Thus, the results indicated that the rate-limiting step was the diffusion of the liquid film in the adsorption process [22].

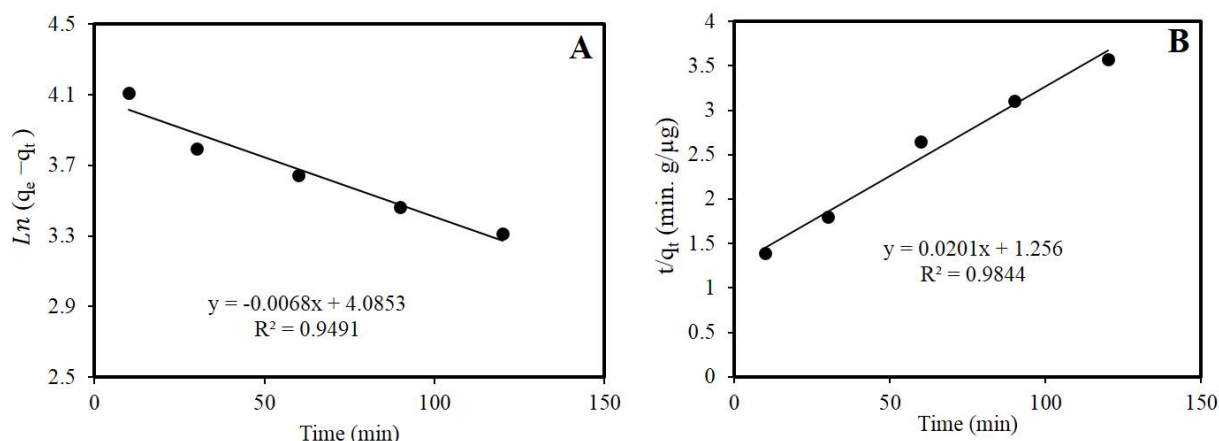


Fig 7 Plots of pseudo-first (A) and pseudo-second (B) order kinetic models of ZEN adsorption on silica NPs

Table 1 Parameters of kinetic models in ZEN adsorption by SNPs

Sorbsent	Pseudo-first-order			Pseudo-second-order		
	Regression equation	k ₁ (min ⁻¹)	R ²	Regression equation	k ₂ (g μg ⁻¹ min ⁻¹)	R ²
Silica NPs	Ln (q _e - q _t) = 4.0853 - 0.0068 t	0.0068	0.9491	t/q _t = 1.256 + 0.0201 t	0.00021	0.9844

3-7- Adsorption Isotherms

Isotherms play a crucial role in the evaluation of adsorption processes, as they provide key insights into the distribution of the target species between the adsorbent phase (solid) and the solution containing the analyte (liquid phase) once equilibrium has been reached. To assess the equilibrium isotherms during the adsorption process, the Langmuir and Freundlich models are commonly used [22]. The homogeneous distribution of the adsorbent surface with similar sites is analyzed using the Langmuir model, which is described by the following equation:

$$C_e/q_e = C_e/q_m + 1/K_L q_m \tag{5}$$

where C_e is the equilibrium concentration of a substance in the solution (μg/l), q_e is the amount of ZEN per gram of adsorbent under equilibrium conditions (μg/g), q_m is the maximum amount of ZEN per gram of adsorbent (μg/g) and Langmuir constant K_L (l/ μg) is The linear graph of C_e/q_e versus C_e in Figure A 8 can be used to measure q_m and K_L parameters.

By showing the surface as diverse adsorption sites and heterogeneous distribution, the Freundlich model is used as a multi-layer adsorption model on the surface of adsorbents based on the following relationship:

$$q_e = K_F C_e^{1/n} \tag{6}$$

The above equation is presented in linear mode with the following equation:

$$\ln q_e = \ln K_F + 1/n \ln C_e$$

where q_e is the amount of ZEN per gram of adsorbent in equilibrium conditions ($\mu\text{g/g}$), K_F is the Freundlich constant (g/l), n is the absorption intensity and C_e is the equilibrium concentration of a substance in the solution ($\mu\text{g/l}$). Based on the linear graph of $\ln q_e$ versus $\ln C_e$, as shown in Figure B8, the K_F and n parameters can be calculated.

Adsorbent performance was evaluated according to the above models by adding 4 mg of SNPs to 25 $\mu\text{g/L}$ of ZEN as the initial concentration for 240 minutes. ZEN residual concentration was measured by HPLC and parameters were calculated in Freundlich and Langmuir models (Table 2). These results showed that under the studied experimental conditions, ZEN adsorption on SNPs showed the best agreement with the Freundlich model due to the high correlation coefficient. Based on this, the Freundlich model was recognized as a suitable model to evaluate ZEN adsorption equilibrium on SNPs, which presented a multilayered and heterogeneous surface in the adsorption process.

Previous studies on modeling the reduction or removal of mycotoxins, particularly

afatoxins, are diverse and employ various approaches for modeling and predicting these processes [25]. Some studies have focused on the kinetics of adsorption and desorption of different adsorbents for aflatoxins, while others have used mathematical models to simulate and predict aflatoxin removal [26, 27]. A study by Hashemi and Amir in 2020 demonstrated that modeling using the Langmuir and Freundlich models could effectively describe the adsorption of Aflatoxin B1 by graphene oxide nanoparticles, aligning well with experimental data [28]. Additionally, Abbasi et al. (2021) showed that magnetic graphene oxide nanocomposites (MGO) are effective for the simultaneous removal of Aflatoxin B1 (AFB1) and Ochratoxin A (OTA). Optimization conditions using response surface methodology revealed that optimizing pH, time, and temperature were effective in the adsorption of these mycotoxins. The pseudo-second-order kinetic model and Freundlich isotherm were well-matched with experimental data, indicating that the adsorption of these mycotoxins occurs through physical interactions such as hydrogen bonding, π - π stacking, electrostatic, and hydrophobic interactions.

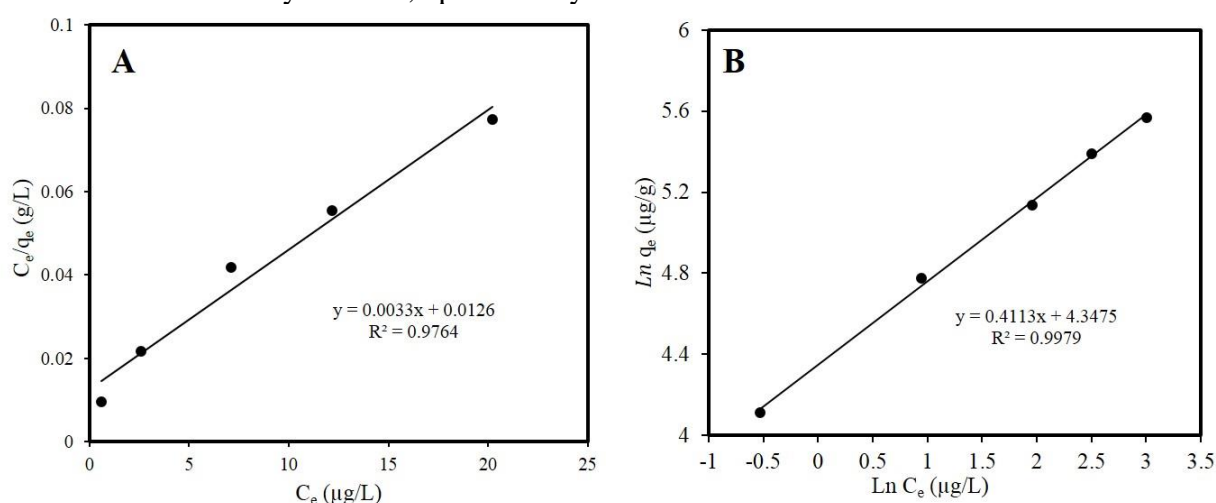


Fig 8 Plots of Langmuir isotherm (A) and Freundlich isotherm (B) models of SNPs for ZEN adsorption.

Table 2 Langmuir and Freundlich isotherm constants in ZEN adsorption by SNPs

Sorbent	Langmuir isotherm model			Freundlich isotherm model		
	q_m ($\mu\text{g/g}$)	K_L ($\text{L } \mu\text{g}^{-1}$)	R^2	K_F ($\mu\text{g g}^{-1}$)($\text{L } \mu\text{g}^{-1}$) ^{1/n}	n	R^2
SNPs	303.03	0.262	0.9764	77.29	2.431	0.9979

3-8- Degradation of ZEN by UV Radiation

To address mycotoxins, UV radiation is recognized as a highly effective physical method due to its long-term photoreactivity. UV radiation offers advantages as a non-thermal method for food decontamination, including environmental compatibility, cost-effectiveness, and practicality, while also not producing toxic by-products or waste [22]. The effectiveness of this process depends on parameters such as exposure time and radiation intensity. In this study, UV treatment at 265 nm reduced ZEN levels by 98.81% after 180 minutes of exposure (Figure 9). The detoxification mechanism through UV light relies on breaking chemical bonds in macromolecules, resulting in the formation of smaller molecular units. Although the exact mechanism of ZEN reduction and inactivation by UV light is not fully understood, it may be due to the degradation of the toxin's structure into non-toxic or less toxic fragments.

Overall, based on reported results, low levels of UV radiation do not significantly impact the sensory and physicochemical properties of food products [22]. UV radiation can easily penetrate transparent liquids but has limited penetration into solid materials. Therefore, the detoxification efficiency in food products containing high amounts of suspended solids is lower [22]. Consequently, for UV detoxification experiments, non-transparent or powdered food products should be used in thin layers [22].

Morita et al. investigated the effects of weak UV (0.1 mW cm^2) and strong UV (24 mW cm^2) radiation for reducing ZEN levels. In their study, ZEN (30 mg/kg) was completely reduced by strong UV radiation in 15 minutes and by weak UV radiation in 60 minutes [22]. In another study, 62 to 79% of ZEN in corn kernels was reduced after exposure to UV light at 15 J/cm^2 [22]. In the present study, ZEN levels were significantly reduced by 98.81% with UV radiation at 265 nm over 180 minutes.

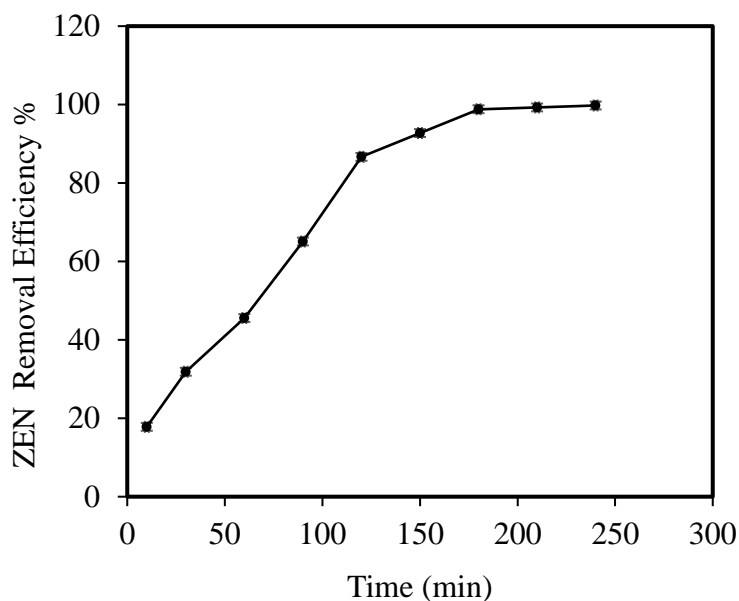


Fig 9 Effect of UV irradiation on ZEN adsorption with variation of time

3-9- Quantitative Determination of ZEN in Sunflower Oil Samples

To evaluate the effectiveness of the new detoxification method using SNPs, a pure sunflower oil sample was spiked with 25 $\mu\text{g/L}$ of ZEN and compared with UV radiation treatment. Based on optimal conditions and exposure times, the removal efficiency of ZEN by SNPs and UV radiation was estimated to be 92.1% in 240 minutes and 96.22% in 180 minutes, respectively. The results demonstrated that ZEN is highly sensitive to both SNPs and UV radiation, showing a high removal efficiency in sunflower oil samples.

4- Conclusion

In this study, the effects of SNPs as an adsorbent and UV radiation on ZEN-contaminated sunflower oil samples were investigated. The pure sunflower oil sample did not show any ZEN contamination. The optimal conditions for ZEN removal by SNPs were found to be a contact time of 240 minutes with an initial ZEN concentration of 25 $\mu\text{g/L}$ and 4 mg of SNPs.

Additionally, kinetic data aligned well with the Freundlich model and the pseudo-second-order kinetic model. These results indicate that SNPs have a high adsorption capacity and can serve as an effective adsorbent for ZEN removal from sunflower oil. The study confirmed that SNPs were significantly more effective in reducing ZEN levels compared to UV radiation. It was found that the adsorption process is more compatible with the Freundlich model, indicating that ZEN adsorption by SNPs occurs through multiple-site interactions at the surface and within the layers of the silica structure. The likely adsorption mechanism involves the specific chemical reactions between the functional groups of zearalenone and the silica groups, leading to efficient chemical adsorption of ZEN. Overall, the chemical interactions with SNPs' functional groups, combined with the particles' porosity, appear to be the main mechanisms for ZEN adsorption on the adsorbent surface. The use of SNPs was more effective than UV radiation in reducing ZEN levels. Selecting the most cost-effective method for removing contaminants from contaminated feed products is crucial. This work highlights that using an adsorbent like SNPs is a more effective and economical approach for aflatoxin removal. SNPs also reduced ZEN

levels in a time-dependent manner but at a faster rate. Therefore, it was confirmed in laboratory conditions that SNPs are effective in reducing ZEN levels. The synthesized SNPs did not exhibit any toxic or detrimental effects on food and, due to their unique properties such as fine pore size, hydrophilicity, and very high adsorption capacity due to their significant surface-to-volume ratio, could be introduced as a new material for film production in the food packaging and preservation industry. Consequently, this method could serve as an effective approach for significant ZEN removal from natural samples like edible oils.

5-References

- [1] Ahmadi M, Jahed Khaniki G, Shariatifar N, Molaee-Aghaee E. Investigation of aflatoxins level in some packaged and bulk legumes collected from Tehran market of Iran. *International Journal of Environmental Analytical Chemistry*. 2022;102(16):4804-13.
- [2] Fakhri Y, Ghorbani R, Taghavi M, Keramati H, Amanidaz N, Moradi B, et al. Concentration and prevalence of aflatoxin M1 in human breast milk in Iran: Systematic review, meta-analysis, and carcinogenic risk assessment: A review. *Journal of food protection*. 2019;82(5):785-95.
- [3] Babakhanian A, Momeneh T, Aberoomand-azar P, Kaki S, Torki M, Kiaie SH, et al. A fabricated electro-spun sensor based on Lake Red C pigments doped into PAN (polyacrylonitrile) nano-fibers for electrochemical detection of Aflatoxin B1 in poultry feed and serum samples. *Analyst*. 2015;140(22):7761-7.
- [4] Richard JL. Some major mycotoxins and their mycotoxicoses—An overview. *International journal of food microbiology*. 2007;119(1-2):3-10.
- [5] Gazzah AC, Camoin L, Abid S, Bouaziz C, Ladjimi M, Bacha H. Identification of proteins related to early changes observed in Human hepatocellular carcinoma cells after treatment with the mycotoxin Zearalenone. *Experimental and toxicologic pathology*. 2013;65(6):809-16.
- [6] Poór M, Kunsági-Máté S, Bálint M, Hetényi C, Gerner Z, Lemli B. Interaction of mycotoxin zearalenone with human serum albumin. *Journal of Photochemistry and Photobiology B: Biology*. 2017;170:16-24.
- [7] Akhavan-Mahdavi S, Mirzazadeh M, Alam Z, Solaimanimehr S. The effect of chitosan coating combined with cold plasma on the quality and safety of pistachio during storage. *Food Science & Nutrition*. 2023;11(7):4296-307.
- [8] Noroozi R, Sadeghi E, Rouhi M, Safajoo S, Razmjoo F, Paimard G, et al. Fates of aflatoxin B1 from wheat flour to Iranian traditional cookies: Managing procedures to aflatoxin B1 reduction during traditional processing. *Food science & nutrition*. 2020;8(11):6014-22.
- [9] Zhang W, Zhang S, Wang J, Dong J, Cheng B, Xu L, et al. A novel adsorbent albite modified with cetylpyridinium chloride for efficient removal of zearalenone. *Toxins*. 2019;11(11):674.
- [10] Poór M, Faisal Z, Zand A, Bencsik T, Lemli B, Kunsági-Máté S, et al. Removal of zearalenone and zearalenols from aqueous solutions using insoluble beta-cyclodextrin bead polymer. *Toxins*. 2018;10(6):216.
- [11] Wu N, Ou W, Zhang Z, Wang Y, Xu Q, Huang H. Recent advances in detoxification strategies for zearalenone contamination in food and feed. *Chinese Journal of Chemical Engineering*. 2021;30:168-77.
- [12] Wang N, Wu W, Pan J, Long M. Detoxification strategies for zearalenone using microorganisms: A review. *Microorganisms*. 2019;7(7):208.
- [13] Tan H, Guo T, Zhou H, Dai H, Yu Y, Zhu H, et al. A simple mesoporous silica nanoparticle-based fluorescence aptasensor for the detection of zearalenone in grain and cereal products. *Analytical and bioanalytical chemistry*. 2020;412:5627-35.
- [14] Savi GD, Torres Zanoni E, Scussel R, Córneo EdS, Guimarães Furtado B, Macuvele DLP, et al. Mesoporous silica nanoparticles adsorb aflatoxin B1 and reduce mycotoxin-induced cell damage. *Journal of Environmental Science and Health, Part B*. 2023;58(1):1-9.

- [15] Horky P, Skalickova S, Baholet D, Skladanka J. Nanoparticles as a solution for eliminating the risk of mycotoxins. *Nanomaterials*. 2018;8(9):727.
- [16] Liu M, Zhao L, Gong G, Zhang L, Shi L, Dai J, et al. Invited review: Remediation strategies for mycotoxin control in feed. *Journal of Animal Science and Biotechnology*. 2022;13(1):19.
- [17] Haidukowski M, Casamassima E, Cimmarusti MT, Branà MT, Longobardi F, Acquafredda P, et al. Aflatoxin B1-adsorbing capability of *Pleurotus eryngii* mycelium: efficiency and modeling of the process. *Frontiers in Microbiology*. 2019;10:1386.
- [18] Kifer D, Jakšić D, Šegvić Klarić M. Assessing the effect of mycotoxin combinations: which mathematical model is (the most) appropriate? *Toxins*. 2020;12(3):153.
- [19] Raesi S, Mohammadi R, Khammar Z, Paimard G, Abdalbeygi S, Sarlak Z, et al. Photocatalytic detoxification of aflatoxin B1 in an aqueous solution and soymilk using nano metal oxides under UV light: Kinetic and isotherm models. *Lwt*. 2022;154:112638.
- [20] Nicolau-Lapeña I, Rodríguez-Bencomo JJ, Colás-Medà P, Viñas I, Sanchis V, Alegre I. Ultraviolet applications to control patulin produced by *Penicillium expansum* CMP-1 in apple products and study of further patulin degradation products formation and toxicity. *Food and Bioprocess Technology*. 2023;16(4):804-23.
- [21] Garcia D, Ramos AJ, Sanchis V, Marín S. Modeling kinetics of aflatoxin production by *Aspergillus flavus* in maize-based medium and maize grain. *International journal of food microbiology*. 2013;162(2):182-9.
- [22] Buckley A, Greenblatt M. The sol-gel preparation of silica gels. *Journal of chemical education*. 1994;71(7):599.
- [23] Al-Harbi T, Al-Hazmi F, Mahmoud WE. Synthesis and characterization of nanoporous silica film via non-surfactant template sol-gel technique. *Superlattices and Microstructures*. 2012;52(4):643-7.
- [24] Zhao Z, Liu N, Yang L, Wang J, Song S, Nie D, et al. Cross-linked chitosan polymers as generic adsorbents for simultaneous adsorption of multiple mycotoxins. *Food Control*. 2015;57:362-9.
- [25] Aguilar-Zuniga K, Laurie VF, Moore-Carrasco R, Ortiz-Villeda B, Carrasco-Sánchez V. Agro-industrial waste products as mycotoxin biosorbents: a review of in vitro and in vivo studies. *Food Reviews International*. 2023;39(5):2914-30.
- [26] Jard G, Liboz T, Mathieu F, Guyonvarc'h A, Lebrihi A. Review of mycotoxin reduction in food and feed: from prevention in the field to detoxification by adsorption or transformation. *Food Additives & Contaminants: Part A*. 2011;28(11):1590-609.
- [27] Pourmohammadi K, Sayadi M, Abedi E, Mousavifard M. Determining the adsorption capacity and stability of Aflatoxin B1, Ochratoxin A, and Zearalenon on single and co-culture *L. acidophilus* and *L. rhamnosus* surfaces. *Journal of Food Composition and Analysis*. 2022;110:104517.
- [28] Hashemi SMB, Amiri MJ. A comparative adsorption study of aflatoxin B1 and aflatoxin G1 in almond butter fermented by *Lactobacillus fermentum* and *Lactobacillus delbrueckii* subsp. *lactis*. *LWT*. 2020;128:109500.



بررسی تاثیر نانوذرات سیلیکا و فرایند فرابنفش بر میزان سم‌زدایی زیرالنون در روغن‌های آفتابگردان

ندا غفاری^۱، احسان صادقی^{۲*}، نسرین چوبکار^۳

- ۱- گروه مواد غذایی، واحد کرمانشاه، دانشگاه آزاد اسلامی، کرمانشاه، ایران
۲- مرکز تحقیقات عوامل محیطی موثر بر سلامت دانشگاه علوم پزشکی کرمانشاه، کرمانشاه، ایران
۳- مرکز تحقیقات بیوتکنولوژی گیاهی، واحد کرمانشاه، دانشگاه آزاد اسلامی، کرمانشاه، ایران

اطلاعات مقاله	چکیده
تاریخ های مقاله : تاریخ دریافت: ۱۴۰۲/۱۲/۱۵ تاریخ پذیرش: ۱۴۰۳/۴/۱۳	در این مطالعه، اثر نانوذرات سیلیکا (SNPs) و تابش UV بر حذف زیرالنون (ZEN) از روغن آفتابگردان بررسی شد. نمونه روغن آفتابگردان خالص آلودگی به ZEN را نشان نداد. بهترین شرایط برای حذف ZEN توسط SNPs در زمان تماس ۲۴۰ دقیقه، غلظت اولیه ZEN برابر با ۲۵ میکروگرم بر لیتر، و مقدار ۴ میلی گرم SNPs تعیین شد. داده‌های سینتیکی مطابق مدل فروندلیچ و مدل شبه مرتبه دوم بودند. نتایج نشان داد که SNPs ظرفیت جذب بالایی داشته و به عنوان یک جاذب مناسب برای حذف ZEN در روغن آفتابگردان عمل می‌کنند. تاثیر SNPs در کاهش ZEN بسیار موثرتر از تابش UV بود. مکانیسم جذب احتمالی شامل پیوند شیمیایی گروه عملکردی ZEN با گروه‌های سیلیکا و تخلخل بالای SNPs می‌باشد. استفاده از SNPs به دلیل هزینه کم و عدم اثر سمی، روش موثری برای حذف ZEN از محصولات غذایی معرفی شد. این روش می‌تواند به عنوان یک راهکار موثر برای حذف ZEN در نمونه‌های طبیعی مانند روغن خوراکی مورد استفاده قرار گیرد.
کلمات کلیدی: نانوذرات سیلیکا، زیرالنون، روغن آفتابگردان، تابش UV، جذب سطحی	
DOI:10.22034/FSCT.21.157.31. * مسئول مکاتبات: ehsan.sadeghi59@yahoo.com	